

# Thermal, mineralogical and spectroscopic study of plasters from three post-Byzantine churches from Kastoria (northern Greece)

Andreas Iordanidis · Javier Garcia-Guinea ·  
Aggeliki Strati · Amalia Gkimourtzina ·  
Androniki Papoulidou

Received: 7 May 2010 / Accepted: 14 September 2010 / Published online: 8 October 2010  
© Akadémiai Kiadó, Budapest, Hungary 2010

**Abstract** Several plaster samples were collected from the wall paintings of post-Byzantine monuments from Kastoria town, northern Greece. They were analysed mainly by simultaneous thermal analysis (TG-DTG/DTA) and X-ray diffraction and supplementary by electron microscope (ESEM-EDX) and Raman spectroscopy. Whitish and dark plaster layers were evident in most cases. Calcite, micas, and quartz were the dominant minerals, while dolomite, gypsum, and feldspar were detected as minor phases in most of the samples. Hydromagnesite and chlinochlore were also determined in a few samples. The utilisation of the results for chronological purposes (i.e. for assignment of different painting periods) was also suggested and the presence of dolomite and hydromagnesite could be characteristic for the provenance of the raw material. Gypsum was regarded mainly as a weathering product due to sulfation process, and secondly as a binding material of the plaster. The thermoanalytical results are in good agreement with the mineralogical data. The white plasters are categorized as hydraulic lime mortars, while the dark ones as natural pozzolanic mortars. Calcite and gypsum correlates well with their respective mass losses at certain temperature ranges and their Raman spectra are clearly detected. ESEM-EDX

revealed fine calcareous components with aluminosilicate aggregates and the application of the fresco technique either as a multi-layer or a single-layer plaster. The deterioration caused by salts (gypsum, halite, and nitratine) and micro-organisms was also determined. The detrimental effect of the salt crystallization and dissolution was also confirmed using the so-called Peltier-stage experiment.

**Keywords** TG/DTG-DTA · Byzantine plasters · XRD · ESEM-EDX · Raman

## Introduction

The chemical, mineralogical and structural characterisation of historic mortars can shed light to the provenance of raw materials and the technological practice, but can also help in the restoration and preservation processes of the architectural heritage. The employment of various physicochemical techniques in the study of mortars is a common practice to cover a wide range of necessary knowledge to perform these renovation. Accordingly, several analytical methods, both destructive and non-destructive, have been used for the qualitative and quantitative characterisation of ancient mortars, like SEM/EDX, FTIR, Raman micro-spectroscopy, DSC/TGA/DTA, microprobe, optical microscopy, XRD, XRF, etc. [1–10]. While several studies have been published regarding pigments and mortars from the Byzantine time [1–3, 11–14], the analytical characterization of the Byzantine and post-Byzantine artefacts of Kastoria, northern Greece, is only sporadically mentioned in the literature [15].

A great development of church architecture and a parallel flourishing of hagiography occurred in the region of Kastoria during Byzantine era. Kastoria was established in the sixth century by the emperor Ioustinianos and has 50

A. Iordanidis (✉)  
Department of Geotechnology and Environmental Engineering,  
Technological Educational Institute (TEI) of Western  
Macedonia, Kila, 50100 Kozani, Greece  
e-mail: aiordanidis@yahoo.co.uk

J. Garcia-Guinea  
Museo Nacional Ciencias Naturales, CSIC, C/José Gutierrez  
Abascal 2, Madrid 28006, Spain

A. Strati · A. Gkimourtzina · A. Papoulidou  
16th Ephorate of Byzantine Antiquities, Mitropoleos 25,  
52100 Kastoria, Greece

preserved temples that belong to Byzantine and post-Byzantine period. Remarkable Byzantine monuments are preserved in Kastoria, with wall paintings with the flawless technique of fresco and rare samples of Byzantine icons and woodcut temples of inestimable artistic value [16].

In this study, the investigation of various post-Byzantine (fourteenth–seventeenth century AD) plasters collected from the wall paintings of three churches from Kastoria town, northern Greece is attempted. The study is focused on the thermal, mineralogical, and chemical characteristics, in an attempt to investigate the raw material used and the technology applied for these types of plasters. Very limited information exists on the analytical characterisation of Kastoria's historic mortars [15], and thus this is the first attempt to study an adequate set of plaster samples. This study is expected to aid curators and archaeologists who are working in the area in their effort to comprehensively study the Byzantine monuments of Kastoria.

## Experimental

### Monuments

Sampling was carried out in three churches, Agios Georgios Vounou, Agios Nikolaos Kyritzi and Agios Nikolaos Magaliou, which are of great interest with commendable artistic meaning. Agios Georgios Vounou was built and decorated with wall paintings in the second half of the fourteenth century, originally as a one-aisle Basilika and it was reconstructed in the sixteenth century and a narthex was added on the northwest side which was also decorated with wall paintings. The wall paintings of Agios Nikolaos Kyritzi are dated in the fourteenth century although the church was expanded towards the south side in a reconstruction that took place in 1654. The one-aisle Basilika church of Agios Nikolaos Magaliou, was decorated with wall paintings in the second half of the fifteenth century, the church also contains wall paintings dated in the seventeenth century which are situated on the east wall. According to the sources both churches Agios Nikolaos Magaliou and Agios Nikolaos Kyritzi were created by the same artist [17].

### Sampling

Plaster samples from the three aforementioned churches were collected from deteriorated areas upon the wall paintings. The samples were dated to post-Byzantine era (fourteenth–seventeenth century AD), and named as GEVO (Agios Georgios Vounou), NIKY (Agios Nikolaos Kyritzi), and NIMA (Agios Nikolaos Magaliou). Two layers were observed in almost all the samples. A whitish layer near the pigmented surface of the wall painting and a

dark one just beneath the whitish layer and both white and dark parts were collected (where possible). Nevertheless, we were only able to collect solely white or dark plaster samples in some cases. The sample characteristics are shown in Table 1. The samples were finely ground for the X-ray diffraction and the thermogravimetric analyses. Moreover, fresh fragments were obtained, where possible, for the ESEM-EDX and Raman analyses.

### Analytical methods

The X-ray diffraction (XRD) technique was employed for the semi-quantitative mineral identification of the ground mortar samples. A Philips PW-1710 powder diffractometer with CuK $\alpha$  radiation was used. Patterns were obtained by step scanning from 3 to 63° 2 $\theta$ , with a goniometer speed of 0.03°/s, operating at 30 kV and 10 mA. The XPOWDER analytical software was used for the semi-quantitative determination of the mineral phases.

A Perkin Elmer STA6000 device was used for the thermogravimetric analysis (TG/DTG-DTA). Approximately 10 mg of powdered mortars were placed in aluminum crucibles. The temperature program ranged from 50 to 1000 °C, at a heating rate of 10 °C min $^{-1}$  under nitrogen atmosphere.

Fractured mortars collected from deteriorated areas of the wall paintings of the three Byzantine churches and polished sections were prepared for the ESEM-EDX analysis. A Philips QUANTA 200 Environmental Scanning Electron Microscope (ESEM), coupled with an Oxford INCA Energy 200 Energy Dispersive System (EDS) was used. It should be noted, however, that only a few samples were analysed by ESEM-EDX and the analysis was restricted within the 2-mm thick layer beneath the pigmented surface.

Additionally, various plaster fragments were also analysed by ESEM-EDX and Raman spectroscopy. Emphasis was given on the pigments, but distinct particles under the pigmented surface of the mortars were also determined. A Thermo Scientific DXR Raman Microscope with a 780 nm laser beam was used, setting the power value of the sample irradiation at 12 mW. The average spectral resolution in the Raman shift range of 100–3000 cm $^{-1}$  was 5 cm $^{-1}$  (grating 400 lines/mm, spot size 2  $\mu$ m). Raman images were obtained using the 20 $\times$  objective of the con-focal microscope. Other analytical parameters were as follows: 30 s bleaching time; 5 exposures of 10 s exposure time.

## Results and discussion

### X-ray diffraction

The mineralogical composition of the analysed plasters is shown in Table 2. Calcite [CaCO<sub>3</sub>] is the most common

**Table 1** Characteristics of the mortar samples collected from the three Byzantine churches of Kastoria, northern Greece

Sample ID and macroscopic color	Chronology	Sampling point in the church	Analytical method applied
GEVO-1	14th c. AD	Eastern wall, sanctuary, right of the apse	ESEM/EDX on cross-section
GEVO-3 WHITE	14th c. AD	Northern wall, sanctuary	TG/DTA, XRD
GEVO-5 WHITE	14th c. AD	Eastern wall, sanctuary	TG/DTA, XRD
GEVO-9 WHITE	14th c. AD	Northern wall, nave, upper painting zone	TG/DTA, XRD
GEVO-10	17th c. AD	Fragment from the sanctuary's floor	ESEM/EDX on cross-section
GEVO-11 WHITE	16th c. AD	Northern wall, narthex	TG/DTA, XRD
GEVO-12	17th c. AD	Fragment from the sanctuary's floor	ESEM/EDX on surface
NIKY-1	14th c. AD	Apse of sanctuary/Lazure	ESEM/EDX on cross-section
NIKY-3 DARK	14th c. AD	Left apse of sanctuary	TG/DTA, XRD
NIKY-3 WHITE	14th c. AD	Left apse of sanctuary	TG/DTA, XRD
NIKY-4 BROWN	14th c. AD	Right apse of sanctuary	TG/DTA, XRD
NIKY-4 WHITE	14th c. AD	Right apse of sanctuary	TG/DTA, XRD
NIKY-5 BROWN	14th c. AD	Eastern and northern wall joint	TG/DTA, XRD
NIKY-5 WHITE	14th c. AD	Eastern and northern wall joint	TG/DTA, XRD
NIKY-7	17th c. AD	Lower part of sanctuary's wall	ESEM/EDX on surface
NIKY-8	17th c. AD	Fragment from the sanctuary's floor	ESEM/EDX of surface
NIKY-9 DARK	17th c. AD	Fragment from the sanctuary's floor	TG/DTA, XRD
NIKY-9 WHITE	17th c. AD	Fragment from the sanctuary's floor	TG/DTA, XRD
NIKY-11 WHITE	17th c. AD	Below gauze in lower painting zone	TG/DTA, XRD, ESEM/EDX on cross-section
NIMA-3 BROWN	17th c. AD	Eastern wall, sanctuary	TG/DTA, XRD
NIMA-6 BROWN	17th c. AD	Southern wall, sanctuary	TG/DTA, XRD
NIMA-7 DARK	15th c. AD	Northern wall, nave	TG/DTA, XRD

GEVO Agios Georgios Vounou, NIKY Agios Nikolaos Kyritzi, NIMA Agios Nikolaos Magaliou

mineral found in all the samples, with concentrations ranging from 60.8 to 91.6% for the white plasters and between 3.1 and 29.2% for the dark samples. Micas (mainly ascribed to muscovite  $[KAl_3Si_3O_{10}(OH,F)_2]$ ) are also determined with a range of concentrations between 5.5 and 9.3% for the white plasters and between 18.3 and 68.1% for the dark ones. Quartz  $[SiO_2]$  phases are also common in all the samples with higher concentrations in dark plasters (3.4–58.9%) and lower in the whitish ones (0.5–19.5%). The extremely high concentration of quartz (58.9%) in sample NIKY-4 BROWN, along with its very low calcite percentage (3.1%) clearly points out that this sample is rather part of the muddy brick substrate of the church's wall than a plaster fragment. Gypsum  $[CaSO_4 \cdot 2H_2O]$  is another abundant mineral derived either from the binder of the plaster or as a deterioration product of the calcite component of the plasters [18]. It is present both in white and dark plasters, having content between 8.3 and 22.7%. Dolomite  $[CaMg(CO_3)_2]$  was also present in several samples with concentrations ranging between 5.2 and 19.7%. Samples NIKY-4 BROWN and NIKY-5 BROWN, having the highest concentrations of dolomite could be regarded as magnesian lime mortars. Moreover, the provenance of dolomite might be related to local magnesium-rich carbonate rocks [12]. Clinochlore

$[(Mg,Fe)_5Al(Si_3Al)O_{10}(OH)_8]$  is apparent in two samples from the Agios Nikolaos Magaliou (NIMA) church. The presence of this mineral in these two plasters and the similarities in their mineralogical composition might indicate that these materials have been applied during the same period and thus they have been erroneously categorized in different periods (fifteenth and seventeenth century AD, respectively). Clicochole has also been found in historic mortars by other scholars [19] and was related to the provenance of local materials. Feldspars  $[(K,Na,Ca)AlSi_3O_8]$ , are present only in two dark samples (NIKY-5 BROWN and NIKY-9 DARK). The percentages of amorphous phases vary between 1.1 and 4.2%. The presence of hydromagnesite  $[Mg_5(CO_3)_4(OH)_2 \cdot 4H_2O]$  in only one sample (NIKY-5 WHITE) is also noticeable, although its small content (1.4%) may attribute it to a decay product from Mg-rich raw material. The development of hydromagnesite results from the hydration and carbonation of MgO in the lime paste in a moist  $CO_2$  atmosphere [12].

#### Thermal analysis (TG-DTG/DTA)

The thermogravimetric (TG) analytical results (mass loss during thermal treatment within certain temperature

**Table 2** Semi-quantitative mineralogical composition of the mortar samples collected from the three Byzantine churches of Kastoria, northern Greece

	GEVO-3 WHITE	GEVO-5 WHITE	GEVO-9 WHITE	NIKY-3 DARK	NIKY-4 WHITE	NIKY-5 BROWN	NIKY-9 WHITE	NIKY-11 BROWN	NIMA-3 BROWN	NIMA-6 BROWN	NIMA-7 DARK
Calcite $\text{CaCO}_3$	91.6	84.5	90.1	62.9	11.3	79.2	3.1	60.8	12.1	87.4	26.3
Dolomite $\text{CaMg}(\text{CO}_3)_2$				19.7			8.5	11.4	5.2	78.3	96.5
Quartz $\text{SiO}_2$	0.8	6.8	0.5	6.6	21.3	19.5	58.9	14.1	25.3	8.7	21.6
Feldspar ( $\text{KNa,CaAlSi}_3\text{O}_8$								12.1	5.7	3.4	22.2
Muscovite $\text{KA}_3\text{Si}_3\text{O}_{10}(\text{OH,F})_2$	5.5	7.6		9.3	54.9		18.3	27.7	32.9	68.1	17.1
Gypsum $\text{CaSO}_4 \cdot 2\text{H}_2\text{O}$										27.8	48.4
Amorphous	1.8	1.1	1.2	1.5	4.2	1.2	1.1	2.5	2.5	1.8	2.0
Clinochlore $(\text{Mg,Fe})_5\text{Al}(\text{Si}_3\text{Al})\text{O}_{10}(\text{OH})_8$									11.0	14.2	11.8
Hydromagnesite $\text{Mg}_5(\text{CO}_3)_4(\text{OH})_2 \cdot 4\text{H}_2\text{O}$									2.5	1.2	2.1
									4.4	3.2	3.2
											1.4

GEVO Agios Georgios Vounou, NIKY Agios Nikolaos Kyritzi, NIMA Agios Nikolaos Magalou

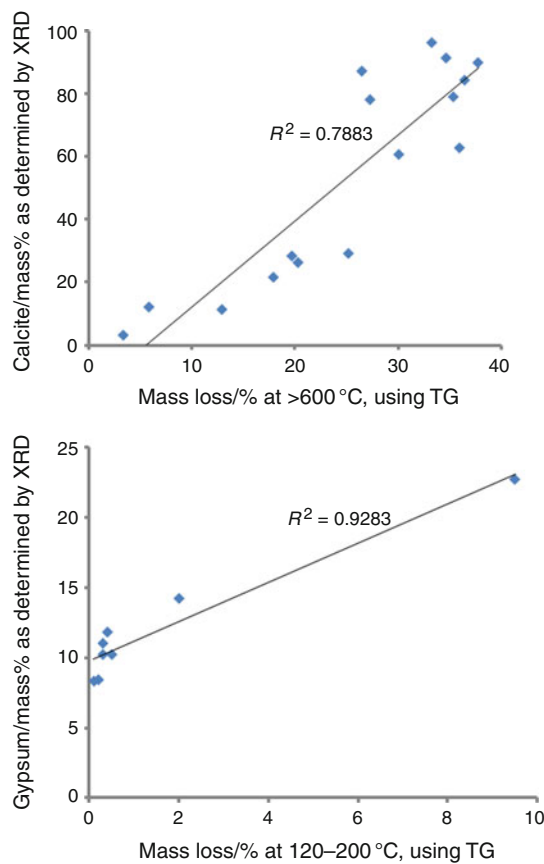
ranges) are shown in Table 3. The total mass loss (%) varies between 7.6 and 55.7%. The lowest mass loss is observed in sample NIKY-4 BROWN, which is apparently not a plaster, but the muddy substrate of the wall paintings. The mass loss between 120 and 200 °C is attributed to the water from hydrated salts, between 200 and 600 °C to the structurally bound water of hydraulic compounds, while the loss above 600 °C is due to the decomposition of carbonates. The  $\text{CO}_2/\text{H}_2\text{O}$  ratio, i.e. mass loss in the temperature range >600 °C over that at the range 200–600 °C, can provide information regarding the hydraulic character of the binder [1, 3, 5, 11, 20–22]. Such values have been determined in our study and are represented in Table 3. Lime mortars have been classified as having  $\text{CO}_2/\text{H}_2\text{O}$  ratio >10, while hydraulic lime mortars have  $\text{CO}_2/\text{H}_2\text{O}$  values between 4 and 10 and pozzolanic mortars have values <3 [3, 22]. According to Cardano et al. [23], the estimation of the hydraulicity of the mortars may be problematic when micas are present, and this is the case of some of our samples. The  $\text{CO}_2/\text{H}_2\text{O}$  values of the plasters in our study vary between 0.75 and 9.45. In general, low values (<1) have been measured for the dark and brown plasters, and are considered as natural pozzolanic mortars, while white plasters exhibit generally values characteristic of hydraulic lime mortars. An exception is the whitish mortar NIKY-4 WHITE, which has a rather low  $\text{CO}_2/\text{H}_2\text{O}$  value of 2.45 and this is attributed to its high calcium sulphate content and sample NIKY-5 WHITE which also reveals low ratio of  $\text{CO}_2/\text{H}_2\text{O}$ , which could be attributed to the presence of hydromagnesite that adds amounts in the structural water range. According to Duran et al. [24] (2008), the ideal value of hydraulic module to obtain high resistance must be between 1.8 and 2.2, and when the value is lower than 1.8 very low resistance is obtained and cracking take place, while values greater than 2.2 are due to a high content of CaO, which produces an excess amount of free CaO.

The correlation of calcite contents (as determined by XRD methodology) and the mass loss (%) at the temperature range >600 °C (as determined by TG, see Table 3) is very good ( $R^2 = 0.79$ ), as shown in Fig. 1. Similarly, the gypsum contents are well correlated ( $R^2 = 0.93$ ) with the mass loss (%) at the temperature range 120–200 °C, fact that supports the widely accepted attribution of these minerals to the mass loss within the temperature range 120–200 °C.

A combined diagram, showing the TG and DTA curve of a characteristic plaster sample (NIKY-4 WHITE) is shown in Fig. 2. The characteristic endothermic peak at 138 °C is ascribed to gypsum hydrated salt, which was found in high contents using XRD method. The endothermic 742 °C peak is due to the decomposition of carbonates. A weak endothermic peak at 870 °C is also observed in the DTA curve, which is attributed to the polymorphic transformation of micaceous minerals [25].

**Table 3** Mass loss/% in various temperature ranges and CO<sub>2</sub>/H<sub>2</sub>O ratios

	<120 °C hygroscopic H <sub>2</sub> O	120–200 °C salts H <sub>2</sub> O	200–600 °C structural water (OH) <sup>-</sup>	>600 °C carbonates CO <sub>2</sub>	Total mass loss	CO <sub>2</sub> /H <sub>2</sub> O
GEVO-3 WHITE	3.4	0.1	9.0	34.7	47.2	3.86
GEVO-5 WHITE	0.1	0.2	4.6	36.5	41.4	7.93
GEVO-9 WHITE	0.2	0.1	4.0	37.8	42.1	9.45
GEVO-11 WHITE	6.3	0.2	9.9	36.0	52.4	3.64
NIKY-3 DARK	0.4	0.2	13.4	12.9	26.9	0.96
NIKY-3 WHITE	0.1	0.1	5.5	35.4	41.1	6.44
NIKY-4 BROWN	0.1	0.5	3.7	3.3	7.6	0.89
NIKY-4 WHITE	3.8	9.5	12.3	30.1	55.7	2.45
NIKY-5 BROWN	0.8	0.3	7.7	5.8	14.6	0.75
NIKY-5 WHITE	0.6	1.0	14.7	26.5	42.8	1.80
NIKY-9 DARK	0.9	0.3	11.0	20.3	32.5	1.85
NIKY-9 WHITE	2.5	2.0	9.3	27.3	41.1	2.94
NIKY-11 WHITE	3.2	0.2	11.5	33.3	48.2	2.90
NIMA-3 BROWN	2.4	0.5	7.3	17.9	28.1	2.45
NIMA-6 BROWN	1.2	0.4	12.0	19.7	33.3	1.64
NIMA-7 DARK	0.4	0.2	8.5	25.2	34.3	2.96

**Fig. 1** Correlation diagrams between the contents (mass%) of specific minerals determined by XRD and the mass loss (mass/%) at certain temperature ranges as obtained by TG: **a** Calcite versus mass loss at >600 °C, **b** Gypsum versus mass loss at 120–200 °C

The derivative thermogravimetric (DTG) curves obtained by the thermal analyses of the studied samples are shown in Fig. 3 for the white plasters and Fig. 4 for the dark and brown plasters, indicating the main peaks found. A clear DTG peak for NIKY-5 WHITE mortar is observed at 479 °C and is probably attributed to the decomposition of hydromagnesite that comprises this specific sample [12, 26, 27]. The peaks below 120 °C are related to the elimination of the adsorbed water, while the peaks from 200 to 600 °C are mainly attributed to the dehydroxylation of structural OH<sup>-</sup> in micas (phyllosilicates). The peaks observed between 730 and 760 °C are associated with the decarboxylation of calcite. Despite the fact that calcite usually decomposes at 750–850 °C, the decrease in the decomposition temperature has been frequently observed in thermoanalysis, especially when we have mixtures of calcite with other impurities (salts, organics, etc.) [25, 28].

The DTG curves of the dark and brown mortars reveal (Fig. 4) characteristic peaks between 691 and 735 °C, attributed to calcite and dolomite decomposition. The peak of NIKY-4 BROWN sample at 630 °C is rather associated with the release of structural water from micas, since the calcite content of this sample is very low. The same sample shows an intensive DTG peak at 117 °C, which is related with the decomposition of gypsum. Only sample NIKY-3 DARK shows a clear DTG peak at 339 °C (i.e. within the range 200–600 °C), which is attributable to dehydroxylation of micaceous minerals.

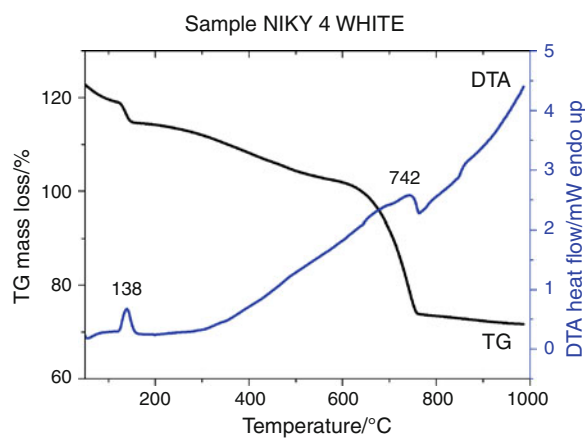


**Fig. 2** Thermal (TG-DTA) curve of a typical Byzantine mortar sample (NIKY-4 WHITE) of this study

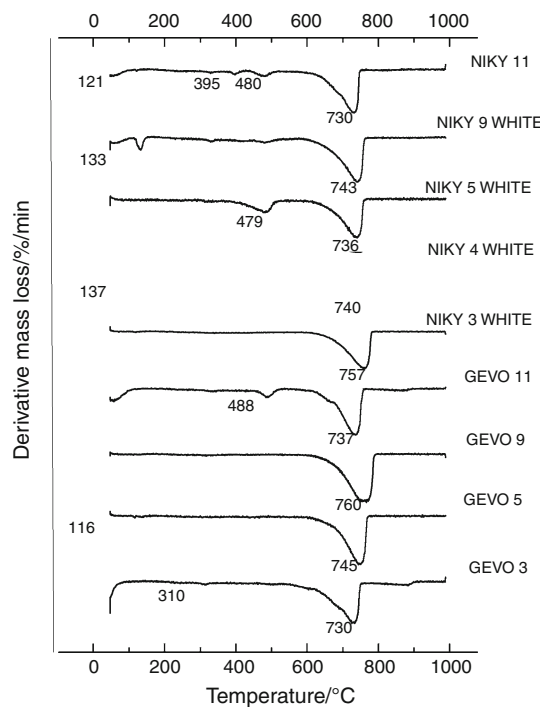


**Fig. 3** DTG curves of all the white Byzantine mortar samples

#### ESEM-EDX

A characteristic ESEM photomicrograph of the cross-section of NIKY11-WHITE sample is shown in Fig. 5. Four distinctive layers are evident (*a*, *b*, *c*, and *d*) and their chemical composition, as revealed by the EDX spectra taken from these areas are also shown in Fig. 5. A Ca-rich structure is obvious for all the layers with minor amounts of silicon ( $\text{SiO}_2$ ), aluminum ( $\text{Al}_2\text{O}_3$ ), and magnesium ( $\text{MgO}$ ). The presence of small amounts of magnesium in the lime mortars has been found previously in other historic mortars [29]. The studied plaster is a characteristic lime

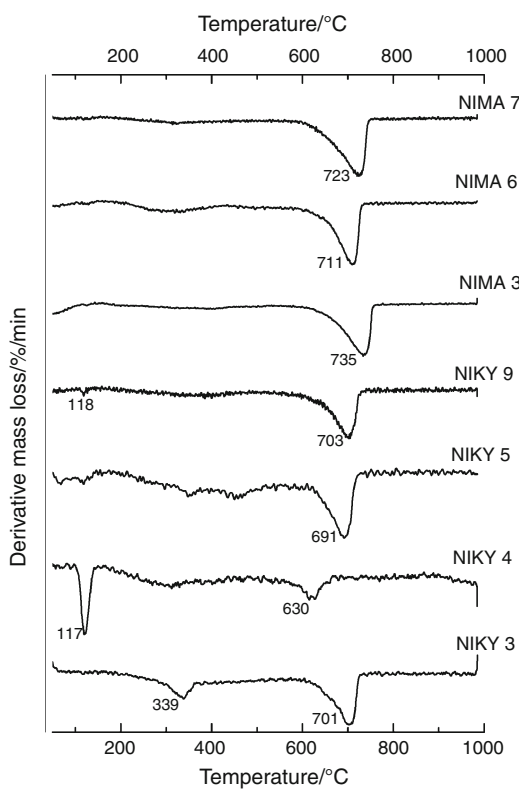
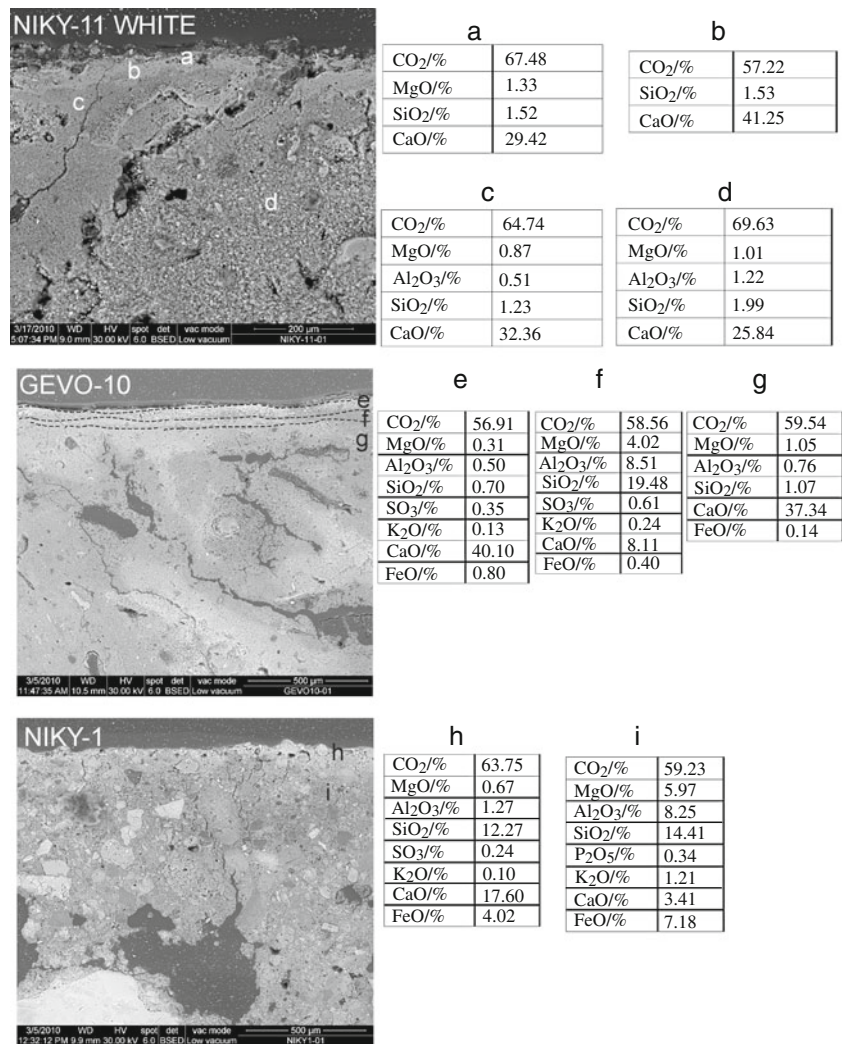


**Fig. 4** DTG curves of all the dark and brown Byzantine mortar samples

plaster which was often used during Byzantine and post-Byzantine era. Sample GEVO-10 shows two fine-grained thin layers (*e* and *f*, apprx. 100 and 50  $\mu\text{m}$  thick) just beneath the outer pigmented surface (Fig. 5). The *e* layer is apparently a calcareous substrate (see Tables *e* and *f* in Fig. 5), while the *f* is rich in aluminosilicates with minor amounts of magnesium. The main body of this mortar (*g* layer) is also Ca-rich. These two mortar samples are composed of several layers applied at the same period, as pointed out by their similar components and were probably used as regularization and finishing coats to improve protection and esthetic appearance of the wall paintings [26]. The micro stratigraphy of the plasters indicates that the fresco technique (i.e. application of the lime-water diluted pigments on damp lime-based plaster) has been used.

Sample NIKY-1 is another characteristic studied mortar in this study. The texture of the coarse grains within the inner layer is inhomogeneous under ESEM (Fig. 5) and shows a very low mixing level, while the opposite is true for the medium and outer layer. Various aggregates are visible and dispersed through the matrix. The chemical composition (EDX) is also variable (see Tables *h* and *i* in Fig. 5) with different concentrations of calcium, aluminosilicates, magnesium and iron. Phosphorous amounts have also been detected. The presence of phosphorous may be related to phosphate salts created by biological processes or

**Fig. 5** ESEM photomicrograph of the cross-sections of characteristic mortar samples (NIKY-11 WHITE, GEVO-10 and NIKY-1) and chemical composition (Tables based on EDX analyses) of their respective *highlighted* layers



to the presence of organic matter (e.g., wool fibers, animal hair) in the mortar [30, 31]. Numerous historic mortars include organic additives, like fibrous plants, animal hair, etc., have been used to lower shrinkage of material during setting [18]. The rather high amounts of iron are also noticeable and might be attributed to Fe-rich micas and clays or iron oxides [28]. Some amounts of the latter could have escaped from the red colored surface of this plaster, in which the fresco technique seems to have been attributed.

Overall, the SEM-EDS analysis of plaster samples from all the churches show that calcium is the element with the highest concentration associated with smaller amounts of magnesium and partially sulphur, attributed to gypsum. One sample (NIKY-4 WHITE) with high amounts of gypsum (as determined by XRD and TG) could be regarded as gypsum-lime mortar. Moreover, the small participation of gypsum in the mortars (grains of gypsum were found scattered in the layers of plaster) in other plasters, may indicate that a small amount of gypsum was probably mixed with lime (CaO) and aggregates.

#### Efflorescence and bio-deterioration

The most common process that leads to the deterioration of the wall paintings is the formation of gypsum during sulphation, which involves the dry deposition reaction between limestone (CaCO<sub>3</sub>) and sulphur dioxide (SO<sub>2</sub>) gas, in the presence of high relative humidity. Another important weathering process is the bio-deterioration due to lichens and other micro-organisms.

The salts found both on the surface and within the main body of the plaster samples were studied with the environmental scanning electron microscopy (ESEM) and Raman spectroscopy. Characteristic images of gypsum (hydrated calcium sulphate), halite (NaCl), and nitranite (NaNO<sub>3</sub>) are shown in Fig. 6a and b. High contents of alkali nitrate, sulphates, and chlorides are known to cause weakened structures and all these salts have been detected in our study [23]. While gypsum and halite are very common salts found on mortars, the presence of nitratine is probably related to the presence of proteinecious material



**Fig. 6** ESEM photomicrographs: **a** Gypsum from the outer surface of a mortar, **b** Nitratine (N), and halite (H), crystallized within the mortar structure, and **c** bio-deterioration from bacteria colonies

(e.g., egg or wax) as a binder agent for the manufacture of plasters [14]. Nitrate salts could be regarded as severe deterioration factors and special attention should be taken for this kind of salts [28, 30].

Strong deterioration of wall paintings is often caused by the growth of fungal colonies and other microorganisms like algae and lichens. These organisms generate organic acids which act as atmospheric pollutants [18]. The problem of bio-deterioration of the plasters is addressed on Fig. 6c and attests the importance of biological micro-organisms (bacteria) in the weathering phenomena of plasters in Byzantine monuments. These bacteria have been developed on an iron-rich pigmented surface (NIKY-7 sample) as have been attested by EDX analysis. Iron is

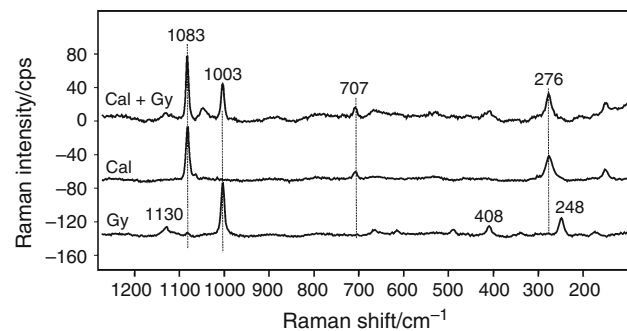


**Fig. 7** Raman spectra of two characteristic mineral phases consisted the mortar samples of this study. *Cal* calcite, *Gy* gypsum (Laser wavelength 780 nm)

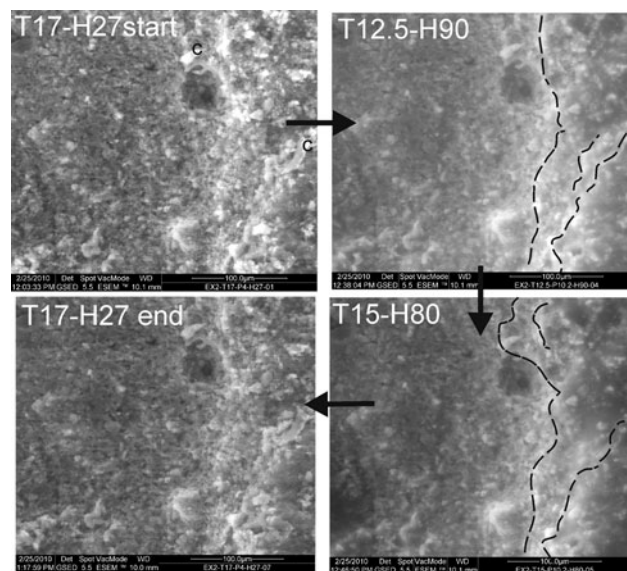


**Fig. 8** ESEM photomicrographs showing dissolution and crystallization of salts during a Peltier-stage experiment on the surface of GEVO-12 sample. The creation of salt crusts is evident. (*T* temperature/°C, *H* humidity/%, and *C* carbonate minerals that remain stable during the experiment)

vital for all the living organisms and since it is commonly found as ferric ( $Fe^{3+}$ ) iron salts, many organisms such as the bacteria of our study use siderophores, i.e. mechanisms to solubilize  $Fe^{3+}$ , for iron uptake [32].

In the Raman spectra of all the plasters, a common characteristic is the strong presence of calcium carbonate with a small participation of gypsum. Figure 7 displays the Raman shifts of two characteristic minerals comprising the white mortars of this study. Calcite is evident from its main peak at  $1083\text{ cm}^{-1}$  and his secondary peaks at  $276$  and  $707\text{ cm}^{-1}$  [7, 33, 34]. Gypsum shows characteristic peaks at  $1003\text{ cm}^{-1}$  (strongest intensity) and  $1130$ ,  $408$ ,  $248\text{ cm}^{-1}$ . The presence of both mineral phases in a white plaster sample, indicating all the relevant Raman shift assignments, is also shown in Fig. 7.

An ESEM experiment was also performed with the Peltier stage changing the temperature and relative humidity to observe how sulphates and other salts crystallize and dissolve inside the pores and over the surface of one plaster sample. A sample with apparently large amounts of salts (GEVO-12) was selected for this experiment. The temperature and relative humidity (RH) were controlled between 12.5–17 °C and 27–90%, respectively, taking into account that the temperature and humidity ranges within Agios Georgios Vounou (GEVO) church are 8–25 °C and 30–90%, respectively. The formation of crusts in high humidity conditions and the crystallization of salts and the creation of new or the widening of previous pores on the surface during desiccation is well monitored in Fig. 8. This mechanism of flaking due to seasonal climatic changes between hot and dry summers and cold and humid winters was clearly observed.

## Conclusions

TG/DTA, XRD, ESEM/EDX, and Raman spectroscopy were applied for the analytical characterization of several Byzantine plasters from Kastoria, northern Greece. The concluding remarks are as follows: the mineralogical investigation showed that the bulk plaster samples are mainly composed of calcite, quartz, micas, gypsum, dolomite, and feldspars, with minor amounts of clinochlore and hydromagnesite. The presence of clinochlore in two samples of one church may facilitate the dating of the plaster application, while dolomite and hydromagnesite could be characteristic for the provenance of the raw material. Gypsum was regarded as a binding material of the plaster as well as weathering product due to sulphation process. The combination of XRD data and thermoanalytical data, which are in good agreement, provided significant information for a thorough characterization of the whitish and dark plasters. All the white studied mortars could be regarded as hydraulic based on the TG results (relations between mass loss due to CO<sub>2</sub> and H<sub>2</sub>O), while most of the dark mortars are regarded as natural pozzolanic ones. Calcite and gypsum correlates well with their respective mass losses at certain temperature ranges and their Raman spectra are clearly detected. ESEM-EDX supplemented our observations, providing information on the structure and composition of different layers of the mortars, the presence of salts on the surface and the interior of the mortars and the deterioration caused by micro-organisms. Fine calcareous components with aluminosilicate aggregates are evident and the fresco technique was attested either as a multi-layer or a single-layer plaster application. High contents of alkali nitrate, sulphates and chlorides have been detected in our study, salts that are known to cause

weakened structures. Micro-organisms (bacteria) responsible for the deterioration of the mortars are also observed. The detrimental effect of the salt crystallization and dissolution was also confirmed using the so-called Peltier-stage experiment. It is thus evident that this study provides valuable information for the conservation and restoration of the highly damaged mortars of the Kastoria's Byzantine monuments.

**Acknowledgements** We acknowledge the financial support of project CGL2009-09247 of the Spanish Plan Nacional I+D+i and the SYNTHESYS Project ES-TAF-258 of the European Community, giving access to the research infrastructures of the Museo Nacional de Ciencias Naturales (MNCN), Madrid, Spain. The technicians Rafael Gonzales-Martin, Laura Tormo, and Manuel Castillejo Magarin of the MNCN are gratefully acknowledged.

## References

1. Moropoulou A, Bakolas A, Bisbikou K. Characterization of ancient, byzantine and later historic mortars by thermal and X-ray diffraction techniques. *Thermochim Acta*. 1995;269/270:779–95.
2. Moropoulou A, Bakolas A, Bisbikou K. Investigation of the technology of historic mortars. *J Cult Herit*. 2000;1:45–58.
3. Moropoulou A, Bakolas A, Anagnostopoulou S. Composite materials in ancient structures. *Cem Concr Compos*. 2005;27: 295–300.
4. Genestar C, Pons C. Ancient covering plaster mortars from several convents and Islamic and Gothic palaces in Palma de mallorca (Spain). Analytical characterization. *J Cult Herit*. 2003;4:291–8.
5. Middendorf B, Hughes JJ, Callebaut K, Baroni G, Papaianni I. Investigative methods for the characterisation of historic mortars—Part 1: mineralogical characterization. *Mater Struct*. 2005;38: 761–9.
6. Clark RJH. Raman microscopy as a structural and analytical tool in the fields of art and archaeology. *J Mol Struct*. 2007;74–80: 834–6.
7. Edwards HG, Farwell DW. The conservational heritage of wall paintings and buildings: an FT-Raman spectroscopic study of prehistoric, Roman, mediaeval and Renaissance lime substrates and mortars. *J Raman Spectrosc*. 2008;39:985–92.
8. Hernanz A, Gavira-Vallejo JM, Ruiz-Lopez JF, Edwards HGM. A comprehensive micro-Raman spectroscopic study of prehistoric rock paintings from the Sierra de las Cuerdas, Cuenca, Spain. *J Raman Spectrosc*. 2008;39:972–84.
9. Iordanidis A, Garcia-Guinea J, Karamitrou-Mentessidi G. Analytical study of ancient pottery from the archaeological site of Aiani, northern Greece. *Mater Charact*. 2009;60:292–302.
10. Sandrolini F, Franzoni E. Characterization procedure for ancient mortars' restoration: the plasters of the Cavallerizza courtyard in the Ducal Palace in Mantua (Italy). *Mater Charact*. 2010;61: 97–104.
11. Bakolas A, Biscontin G, Moropoulou A, Zendri E. Characterization of structural byzantine mortars by thermogravimetric analysis. *Thermochim Acta*. 1998;321:151–60.
12. Maravelaki-Kalaitzaki P, Bakolas A, Karatasios I, Kilikoglou V. Hydraulic lime mortars for the restoration of historic masonry in Crete. *Cem Concr Res*. 2005;35:1577–86.
13. Anastasiou M, Hasapis Th, Zorba T, Pavlidou E, Chrissafis K, Paraskevopoulos KM. TG-DTA and FTIR analyses of plasters from byzantine monuments in Balkan region, comparative study. *J Therm Anal Calorim*. 2006;84:27–32.

14. Daniilia S, Minopoulou E, Andrikopoulos KS, Tsakalof A, Bairaktari K. From Byzantine to post-Byzantine art: the painting technique of St Stephen's wall paintings at Meteora, Greece. *J Archaeol Sci.* 2008;35:2474–85.
15. Pavlidou E, Arapi M, Zorba T, Anastasiou M, Civici N, Stamati F, Paraskevopoulos KM. Onoufrios, the famous XVI's century iconographer, creator of the "Berati School": studying the technique and materials used in wall paintings of inscribed churches. *Appl Phys A.* 2006;83:709–17.
16. Orlando A. Byzantine monuments of Kastoria; Archeion ton Byzantinon mnimeion tis Ellados, 4 (ABME A'); 1938.
17. Tsigaridas E. The monumental painting of the byzantine churches in Kastoria, In Macedonian Hellenism; Melbourne; 1995. pp. 384–93.
18. Bartz W, Filar T. Mineralogical characterization of rendering mortars from decorative details of a baroque building in Kożuchów (SW Poland). *Mater Charact.* 2010;61:105–15.
19. Bianchini G, Marrocchino E, Vaccaro C. Chemical and mineralogical characterisation of historic mortars in Ferrara (northeast Italy). *Cem Concr Res.* 2004;34:1471–5.
20. Genestar C, Pons C, Mas A. Analytical characterisation of ancient mortars from the archaeological Roman city of Pollentia (Balearic Islands, Spain). *Anal Chim Acta.* 2006;557:373–9.
21. Rizzo G, Megna B. Characterization of mortars from ancient and traditional water supply systems in Sicily. *J Therm Anal Calorim.* 2008;92:173.
22. Gleize PJP, Motta EV, Silva DA, Roman HR. Characterization of historical mortars from Santa Catarina (Brazil). *Cem Concr Compos.* 2009;31:342–6.
23. Cardiano P, Sergi S, De Stefano C, Ioppolo S, Piraino PJ. Investigations on ancient mortars from the basilian monastery of Fragala. *Therm Anal Calorim.* 2008;91:477–85.
24. Duran A, Robador MD, Jimenez de Haro MC, Ramirez-Valle V. Study by thermal analysis of mortars belonging to wall paintings corresponding to some historical buildings of Sevillian art. *J Therm Anal Calorim.* 2008;92:353–9.
25. Papadopoulou DN, Lalia-Kantouri M, Kantirani N, Stratis JA. Thermal and mineralogical contribution to the ancient ceramics and natural clays characterization. *J Therm Anal Calorim.* 2006;84:39–45.
26. Adriano P, Santos Silva A, Veiga R, Mirao J, Candeias AE. Microscopic characterisation of old mortars from the Santa Maria Church in Évora. *Mater Charact.* 2009;60:610–20.
27. Hein A, Karatasios I, Mourelatos D. Byzantine wall paintings from Mani (Greece): microanalytical investigation of pigments and plasters. *Anal Bioanal Chem.* 2009;395:2061–71.
28. Alvarez JI, Navarro I, Garcia Casado PJ. Thermal, mineralogical and chemical studies of the mortars used in the cathedral of Pamplona (Spain). *Thermochim Acta.* 2000;365:177–87.
29. Duran A, Perez-Maqueza LA, Poyato J, Perez-Rodriguez JL. A thermal study approach to Roman age wall painting mortars. *J Therm Anal Calorim.* 2010;99:803–9.
30. Sabbioni C, Zappia G, Ghedini N, Gobbi G, Favoni O. Black crusts on ancient mortars. *Atmos Environ.* 1998;32:215–23.
31. Moropoulou A, Polikreti K, Ruf V, Deodatis G. San Francisco Monastery, Quito, Ecuador: characterisation of building materials, damage assessment and conservation considerations. *J Cult Herit.* 2003;4:101–8.
32. Lindh U. Uptake of elements from a biological point of view. In: Selinus O, et al., editors. *Essentials of medical geology.* Amsterdam: Elsevier; 2005. p. 87–114.
33. Socrates G. Infrared and Raman characteristic group frequencies; tables and charts. Chichester: Wiley; 2001.
34. Smith GD, Clark RJH. Raman microscopy in archaeological science. *J Archaeol Sci.* 2004;31:1137–60.